TITLE

Carmela Filosa

Cover art:
Photography:

A catalogue record is available from the Eindhoven University of Technology Library

ISBN: 978-90-386-3972-7

title

PROEFSCHRIFT

ter verkrijging van de graad van doctor aan de Technische Universiteit Eindhoven, op gezag van de rector magnificus prof.dr.ir. F.P.T. Baaijens, voor een commissie aangewezen door het College voor Promoties, in het openbaar te verdedigen

door

Carmela Filosa

geboren te Torre del greco, Italië

Dit proefschrift is goedgekeurd door de promotoren en de samenstelling van de promotiecommissie is als volgt:

voorzitter:	prof.dr.
1^{e} promotor:	prof.dr. W.L. IJzerman
copromotor:	dr. J.H.M. ten Thije Boonkkamp
leden:	

Het onderzoek of ontwerp dat in dit proefschrift wordt beschreven is uitgevoerd in overeenstemming met de TU/e Gedragscode Wetenschapsbeoefening.

“ ”

Abstract

Keywords:

Contents

List of symbols

$\mathrm{d}\Omega$	Solid angle
θ	Angle between the direction of the solid angle and the normal $\boldsymbol{\nu}$
θ_i	Angle between the incident ray and the normal $\boldsymbol{\nu}$
θ_r	Angle between the reflected ray and the normal $\boldsymbol{\nu}$
θ_t	Angle between the transmitted ray and the normal $\boldsymbol{\nu}$

2

Chapter 1

Introduction

1.1 Motivation

1.2 Methods and results

1.3 Content of this thesis

Chapter 2

Non imaging optics

This chapter provides the notions of illumination optics needed in this thesis. We start explaining the difference between radiometry and photometry. In particular, we focus on the photometric variables defining them both in three and two dimensions. The reflection and refraction laws and the phenomenon of total internal reflection are explained. The last paragraph of the chapter gives a brief introduction of the Fresnel's equations.

2.1 Radiometric and photometric variables

Radiometry is the measurement of the electromagnetic radiation across the entire electromagnetic spectrum. Photometry is the subfield of radiometry that takes into account only the portion of the electromagnetic spectrum corresponding to the visible light, [1]. Radiometry deals with radiometric quantities. An important radiometric quantity is the radiant flux Φ_{r} (unit watt, [W]) which is the total energy emitted from a source or received by a target per unit time:

$$\Phi_{\mathrm{r}} = \frac{\mathrm{d}Q}{\mathrm{d}T}\,, \tag{2.1.1}$$

where Q is the energy and T the time.

In Illumination optics the measurement of light is given in terms of the impression that it gives on the human eyes. Therefore, illumination optics deals with the photometric variables. The most important photometric variables are defined as in the following. The luminous flux Φ (unit lumen, [lm]) is defined as the perceived power of light by the human eye, [2]. The radiant and the luminous flux are related by the luminous efficacy function, unit [lm/W], that tells us how many lumen there are for each Watt of power at a given wavelength. The luminous efficacy reaches its maximum at a wavelength of 555 nm where it is equal to 683 lm/W. We may normalize the luminous efficacy function with its maximum value of 683. This normalized function is the dimensionless luminosity function $\bar{y}(\lambda)$ shown in Figure 2.1 where λ is the wavelength.

The luminous flux corresponding to one Watt of radiation power at any wavelength is given by the product of 683 lm/W and the luminosity function at the same wavelength,

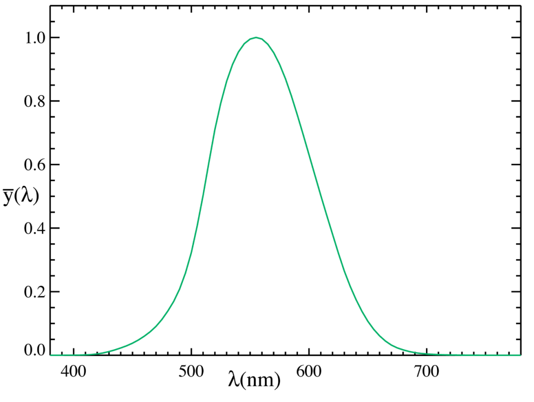

Figure 2.1: Luminosity function $\bar{y}(\lambda)$: relation between the eye's sensitivity and the wavelength of the light. The luminous function is dimensionless.

i.e. $683\,\bar{y}(\lambda)$. Hence, Φ has unit lumen [lm] and it is defined as:

$$\Phi = 683 \int_0^\infty \Phi_\mathrm{r}(\lambda)\bar{y}(\lambda)\mathrm{d}\lambda\ . \tag{2.1.2}$$

The luminous flux $\mathrm{d}\Phi$ falling on a surface is called illuminance E $\big($unit $\big[\mathrm{lm/m^2}\big]\big)$ and is defined as:

$$E = \frac{\mathrm{d}\Phi}{\mathrm{d}A}\ , \tag{2.1.3}$$

where $\mathrm{d}A$ is an infinitesimal area receiving energy.

A beam of light can be described as a collection of light rays, where a light ray can be seen as a path along which the energy travels. The density of light emitted by a point source in a given direction is determined by the solid angle. The solid angle subtended by the light is defined by the infinitesimal surface area $\mathrm{d}A^*$ of a sphere subtended by the radius of that sphere and by the rays emitted by the point source. The solid angle is indicated with Ω and the dimensionless unit of solid angles is the steradian $[sr]$, [3]. Indicating with r the radius of the sphere, the infinitesimal solid angle $\mathrm{d}\Omega$ defined by $\mathrm{d}A$ is given by:

$$\mathrm{d}\Omega = \frac{\mathrm{d}A}{r^2} \tag{2.1.4}$$

The luminous intensity I (unit candela (cd), $[\mathrm{cd} = \mathrm{lm/sr}]$) is defined as the luminous flux $\mathrm{d}\Phi$ per solid angle $\mathrm{d}\Omega$ and is given by:

$$I = \frac{\mathrm{d}\Phi}{\mathrm{d}\Omega}\ . \tag{2.1.5}$$

The luminance L $\big($unit $\big[\mathrm{cd/m^2}\big]\big)$ is the luminous flux per unit solid angle $\mathrm{d}\Omega$ and per unit projected area $\cos(t)\,\mathrm{d}A$ where t is the angle that the normal $\boldsymbol{\nu}$ to area $\mathrm{d}A$ makes with the direction of the solid angle $\mathrm{d}\Omega$, as shown in Figure 2.2. L is given by:

$$L = \frac{\mathrm{d}\Phi}{\cos\theta \mathrm{d}A\mathrm{d}\Omega}. \tag{2.1.6}$$

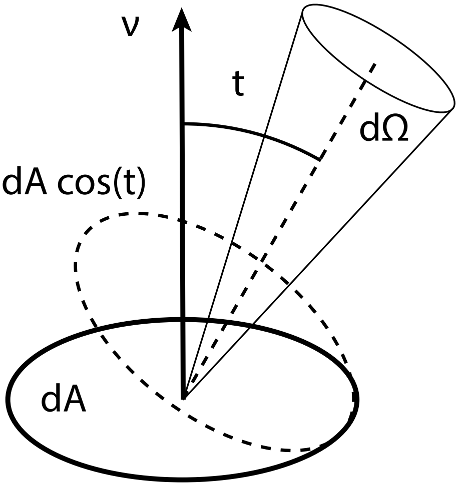

Figure 2.2: Solid angle dΩ in a direction making an angle $\theta$with the normal to the area dA.

Note that from (2.1.5) and (2.1.6) we can derive a relation between the intensity and the luminance.
The infinitesimal intensity dI emitted by the area element dA is given by:

$$\mathrm{d}I = \frac{\mathrm{d}\Phi}{\mathrm{d}\Omega} = L(\mathrm{x}, \theta)\cos(\theta)\mathrm{d}A\,. \tag{2.1.7}$$

When the luminance is uniform over a finite area A, the luminous intensity emitted in the direction $\theta$is equal to:

$$I(t) = L(\theta)A\cos(\theta)\,. \tag{2.1.8}$$

Thus, when $L(\mathrm{x}, \theta)$ does not depend on the position and the direction (i.e. $L(\mathrm{x}, \theta) = L$), we deduce Lambert's cosine law:

$$I(t) = I_0\cos(\theta)\,. \tag{2.1.9}$$

where $I_0 = I(0) = LA$.
Finally the étendue U (unit $[m \cdot srad]$) describes the ability of a source to emitt light or the capability of an optical system to receive light, [4]. The quantity dU is defined as:

$$\mathrm{d}U = n^2\cos(\theta)\mathrm{d}A\mathrm{d}\Omega. \tag{2.1.10}$$

where n is the index of refraction of the medium in which the surface A is immersed. In optics the étendue is considered to be a volume in phase space (or an area for two-dimensional systems). This concept will be clarified in Chapter 4 where we treat the phase space in more details. An important property of the étendue is that it is conserved within an optical system where the flux is constant. We now show, following the same approach used by J. Chaves in [2], how the conservation of this quantity

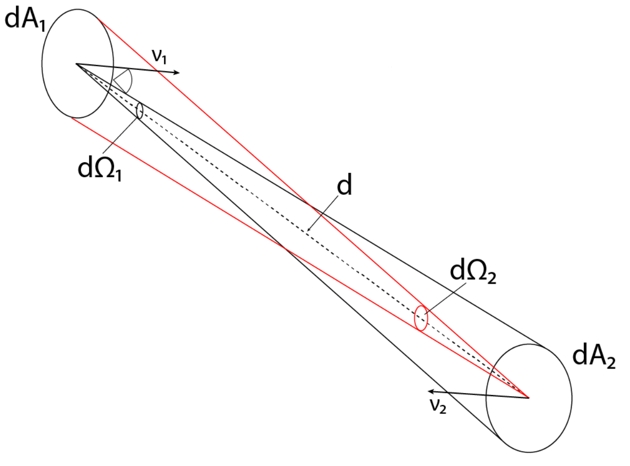

Figure 2.3: $\mathrm{d}A_1$ and $\mathrm{d}A_2$ are two line surfaces with normal ν_1 and ν_2, respectively. t_1 and t_2 are the angles made by the central ray with the normals ν_1 and ν_2, respectively.

can be derived . Consider a light ray emitted from an infinitesimal area $\mathrm{d}A_1$ to the area $\mathrm{d}A_2$ located at a distance d from $\mathrm{d}A_1$, see Figure 2.3.
Indicating with $\boldsymbol{\nu}_1$ and $\boldsymbol{\nu}_2$ the normals to the surfaces $\mathrm{d}A_1$ and $\mathrm{d}A_2$, respectively and with θ_1 and θ_2 the angles that the central ray forms with $\boldsymbol{\nu}_1$ and $\boldsymbol{\nu}_2$, respectively, the flux passing though $\mathrm{d}A_2$ coming from $\mathrm{d}A_1$ is defined as:

$$\mathrm{d}\Phi_1 = L\cos(\theta_1)\mathrm{d}A_1\mathrm{d}\Omega_1 \tag{2.1.11}$$

where $\mathrm{d}\Omega_1$ is defined at the area $\mathrm{d}A_1$ by the area $\mathrm{d}A_2$ and it is given by

$$\mathrm{d}\Omega_1 = \frac{\mathrm{d}A_2\cos(\theta_2)}{d^2}\,. \tag{2.1.12}$$

Similarly, the flux passing though $\mathrm{d}A_1$ coming from $\mathrm{d}A_2$ is equal to:

$$\mathrm{d}\Phi_2 = L\cos(\theta_2)\mathrm{d}A_2\mathrm{d}\Omega_2 \tag{2.1.13}$$

and

$$\mathrm{d}\Omega_2 = \frac{\mathrm{d}A_1\cos(\theta_1)}{d^2}\,. \tag{2.1.14}$$

Then

$$\mathrm{d}U_1 = n^2\mathrm{d}A_1\cos(\theta_1)\mathrm{d}\Omega_1 = \frac{n^2\mathrm{d}A_1\cos(\theta_1)\mathrm{d}A_2\cos(\theta_2)}{d^2}, \tag{2.1.15}$$

and

$$\mathrm{d}U_2 = n^2\mathrm{d}A_2\cos(\theta_2)\mathrm{d}\theta_2 = \frac{n^2\mathrm{d}A_2\cos(\theta_2)\mathrm{d}A_1\cos(\theta_2)}{d^2}\,. \tag{2.1.16}$$

From equation (2.1.15) and (2.1.16) we see that $\mathrm{d}U_1 = \mathrm{d}U_2$. For a light beam, all the light passing through $\mathrm{d}A_1$ coincides with the light passing through $\mathrm{d}A_2$, hence $\mathrm{d}U = \mathrm{d}U_1$. Moreover, for the same light beam, all the light passing from $\mathrm{d}A_2$ corresponds to the light emitted from $\mathrm{d}A_1$, then $\mathrm{d}U = \mathrm{d}U_2$. Finally we can conclude that the étendue $\mathrm{d}U$ is conserved along a beam of light. Since also the flux through the areas $\mathrm{d}A_1$ and $\mathrm{d}A_2$ is conserved, the following relation holds:

$$L := n\frac{\mathrm{d}\Phi}{\mathrm{d}U} = constant\,. \tag{2.1.17}$$

In the optical systems we will consider in this work, the source and the target are located in the same medium (air) with $n = 1$, so the luminance L equals the basic luminance $L^* = L/n$ at the source and the target of the system.

In this thesis we consider two-dimensional optical systems. Hence, we need to find two-dimensional analogies for the definitions given above. In two dimensions the illuminance $\big(\text{unit }[\text{lm/m}]\big)$ denotes the luminous flux falling on an infinitesimal line segment of length $\mathrm{d}x$ and it is given by:

$$E = \frac{\mathrm{d}\Phi}{\mathrm{d}x}\,. \tag{2.1.18}$$

The luminous intensity $\big(\text{unit }[\text{lm/rad}]\big)$ is the luminous flux per angle $\mathrm{d}t$:

$$I = \frac{\mathrm{d}\Phi}{\mathrm{d}\theta}\,. \tag{2.1.19}$$

Thus the following relation holds:

$$\mathrm{d}I = L\cos(t)\mathrm{d}x\,. \tag{2.1.20}$$

The $2D$ luminance $\big(\text{unit }[\text{lm/(rad m)}]\big)$ is given by:

$$L = \frac{\mathrm{d}\Phi}{\cos t\,\mathrm{d}x\,\mathrm{d}\theta}. \tag{2.1.21}$$

The étendue $\mathrm{d}U$ (unit $[m\cdot rad]$) in 2D is given by:

$$\mathrm{d}U = n\cos(\theta)\mathrm{d}a\mathrm{d}\theta. \tag{2.1.22}$$

2.2 Reflection and refraction law

The propagation of a light ray traveling through different media is described by the reflection and refraction law. In this section we introduce these two laws and we explain the total internal reflection phenomenon. A light ray is described by a position vector $\boldsymbol{x}$ and a direction vector $\boldsymbol{t}$ and can be parameterized by the arc length s. Light rays travel in an homogeneous medium along straight lines, once they hit a reflective surface their direction changes. Denoting with $\boldsymbol{t}_i$ the direction of the incident ray and with $\boldsymbol{\nu}$ the unit normal to the surface at the location of the incidence, the direction $\boldsymbol{t}_r$ of the reflected ray is given by:

$$\boldsymbol{t}_r = \boldsymbol{t}_i - 2(\boldsymbol{t}_i, \boldsymbol{\nu})\boldsymbol{\nu}\,, \tag{2.2.1}$$

where the vectors $\boldsymbol{t}_i$ and $\boldsymbol{\nu}$ are unit vectors. From Eq. (2.2.1) it follows that the vector $\boldsymbol{t}_r$ is a unit vector too, indeed considering the scalar product $(\boldsymbol{t}_r, \boldsymbol{t}_i)$ it holds:

$$(\boldsymbol{t}_r, \boldsymbol{t}_i) = (\boldsymbol{t}_r, \boldsymbol{t}_i) - 4(\boldsymbol{t}_r, \boldsymbol{\nu})(\boldsymbol{t}_i, \boldsymbol{\nu}) + 4(\boldsymbol{t}_i, \boldsymbol{\nu})^2(\boldsymbol{\nu}, \boldsymbol{\nu}) = 1. \tag{2.2.2}$$

Denoting the incident angle with θ_i and the reflective angle with θ_r such that

$$\cos\theta_i = -\boldsymbol{t}_i \cdot \boldsymbol{\nu} \qquad \text{and} \qquad \cos\theta_r = \boldsymbol{t}_r \cdot \boldsymbol{\nu}\,, \tag{2.2.3}$$

the reflection law states that θ_i equals θ_r which are measured counterclockwise with respect to the normal $\boldsymbol{\nu}$ of the surface, see Fig. 2.4.

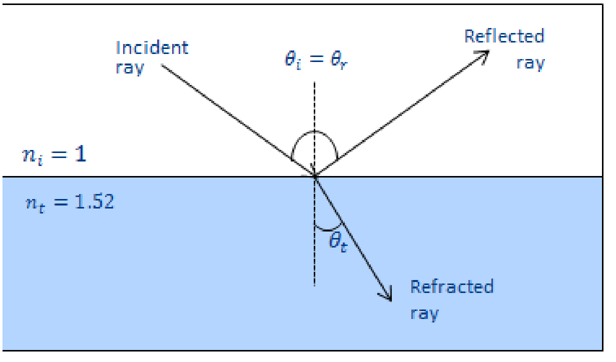

Figure 2.4: $\mathrm{d}A_1$ and $\mathrm{d}A_2$ are two line surfaces with normal ν_1 and ν_2, respectively. t_i and t_2 are the angles made by the central ray with the normals ν_1 and ν_2, respectively.

When a ray propagates through two media with two different media, it direction changes according to refraction law. Indicating with n_i the index of refraction of the medium in which the incident ray travels and with n_t the index of refraction of the medium of the transmitted ray, the direction $\boldsymbol{t}_t$ of the transmitted ray is given by:

$$\boldsymbol{t}_t = n_{i,t}\,\boldsymbol{t}_i + \left[\sqrt{1 - n_{i,t}^2 + n_{i,t}^2(\boldsymbol{\nu},\boldsymbol{t}_i)^2} - n_{i,t}(\boldsymbol{\nu},\boldsymbol{t}_i)\right]\boldsymbol{\nu}\,, \tag{2.2.4}$$

where $n_{i,t} = n_i/n_t$.

Note that in Eq. (2.2.1) the direction of the normal $\boldsymbol{\nu}$ to the surface is not relevant for the computation of the direction of the reflective ray, since:

$$\boldsymbol{t}_r = \boldsymbol{t}_i - 2(\boldsymbol{t}_i,\boldsymbol{\nu})\boldsymbol{\nu} = \boldsymbol{t}_i - 2(\boldsymbol{t}_i,-\boldsymbol{\nu})(-\boldsymbol{\nu}), \tag{2.2.5}$$

while this is not the case of Eq. (2.2.4), therefore in the latter case we need to specify the direction of $\boldsymbol{\nu}$ which is usually chosen in such a way that the angle that it forms with the incident ray $\boldsymbol{t}_i$ is smaller than or equal to $\pi/2$. Hence, if $(\boldsymbol{t}_i,\boldsymbol{\nu}) \geq 0$ the normal $\boldsymbol{\nu}$ directed inside the same medium in which travels the incident ray is taken, otherwise the normal $-\boldsymbol{\nu}$ directed inside the same medium in which the transmitted ray will travel has to be considered.

Eq. (2.2.4) is only valid for

$$\begin{gathered} 1 - n_{i,t}^2 + n_{i,t}^2(\boldsymbol{\nu},\boldsymbol{t}_i)^2 \geq 0 \Rightarrow \frac{n_t}{n_i} \geq \sqrt{1-(\boldsymbol{\nu},\boldsymbol{t}_i)^2} \\ \Rightarrow n_t \geq n_i\sqrt{1-\cos^2(\theta_i)} \Rightarrow n_t \geq n_i \sin(\theta_i) \end{gathered} \tag{2.2.6}$$

The angle for which the equality holds is

$$\theta_\mathrm{c} = \arcsin\left(\frac{n_t}{n_i}\right) \tag{2.2.7}$$

and it is called the critical angle, [2]. Note that the condition $\frac{n_t}{n_i} < 1$ is verified as in this case $\sin(\theta_\mathrm{i}) < 1$. When the incident angle θ_i is exactly equal to the critical angle θ_c the refractive ray propagates parallel to the refractive surface, when $\theta_\mathrm{i} > \theta_\mathrm{c}$ the light ray is no longer refracted but it is reflected by the surface. This phenomenon is called total internal reflection (TIR). When TIR occurs, the 100% of light is reflected and there is no loss of energy. Therefore, optical systems designed such that TIR is always verified are very efficient. In general, light that hits a normal refractive mirror can be both reflected and refracted. Therefore, some part of the energy is transmitted and some part is reflected. The amount of light that is reflected and refracted is determined by the Fresnel's coefficients. In the next paragraph an overview of Fresnel equations is given.

2.3 The Fresnel equations

In order to derive Fresnel's equations we need to describe light as an electromagnetic wave. It is therefore useful to study the light propagation from the perspective of Electromagnetic Theory which gives information about the incident, reflected and transmitted radiant flux density that are denoted with E_i, E_r and E_t, respectively. Any component of the electric field $\boldsymbol{\mathcal{E}}$ can be written in the form

$$\boldsymbol{\mathcal{E}}(\boldsymbol{x}, T) = \boldsymbol{\mathcal{E}}_0(\boldsymbol{x})e^{i(\omega T - \boldsymbol{k}\cdot\boldsymbol{r})} \tag{2.3.1}$$

where the amplitude $\boldsymbol{\mathcal{E}}_0(\boldsymbol{x})$ is constant in time. The vector $\boldsymbol{k}$ has the same direction of the wave and its absolute value $|\boldsymbol{k}| = k = \frac{2\pi}{\lambda}$ is the wave number in vacuum, with λ the wavelength. The value of the angular frequency is $\omega = \frac{ck}{n}$ with c the velocity of the light and n the index of refraction in which the wave is traveling that is the ratio of the speed of light v in the material and the speed of light c in vacuum. Similarly, the magnetic field has the form:

$$\boldsymbol{\mathcal{B}}(\boldsymbol{x}, T) = \boldsymbol{\mathcal{B}}_0(\boldsymbol{x})e^{i(\omega T - \boldsymbol{k}\cdot\boldsymbol{r})}\,. \tag{2.3.2}$$

In the field of electromagnetism a very important concept is the Poynting vector $\boldsymbol{P}$. It defines the energy flux of an electromagnetic field, it is measured in $[W/m^2]$ and it is defined as:

$$\boldsymbol{P} = \frac{1}{\mu}\Big(\mathcal{E} \times \mathcal{B}\Big) \tag{2.3.3}$$

where $\mu = \frac{1}{\varepsilon v^2}$ is the permeability and ε the permittivity. In the following, the vacuum parameters are indicated with the subscript 0. All the quantities defined in the media of the incident, reflective and transmitted light are indicated with the subscripts i, r and t, respectively. Optical rays are perpendicular to the wave front of an electromagnetic wave and parallel to the Poynting vector, [5]. The irradiance E is defined as the average energy that crosses in unit time a unit area A perpedicular to the direction of the energy flow. Therefore:

$$\boldsymbol{E} = <\boldsymbol{P}>_T = \frac{c}{2\mu_0}\boldsymbol{\mathcal{E}}_0^2\,, \tag{2.3.4}$$

where $< \cdot >_T$ indicates the average in time. Considering a beam of light that hit a surface such that an area A is illuminated, the incident, reflected and transmitted beams are $\boldsymbol{E}_i A\cos(\theta_i)$ $\boldsymbol{E}_r A\cos(\theta_r)$ and $\boldsymbol{E}_t A\cos(\theta_t)$, respectively. The reflectance $\mathcal{R}$ is the ratio of the reflected power to the incident power:

$$\mathcal{R} = \frac{\boldsymbol{E}_r A\cos(\theta_r)}{\boldsymbol{E}_i A\cos(\theta_i)} \tag{2.3.5}$$

Similarly, the transmittance T is the ratio between the transmitted to the incident power:

$$\mathcal{T} = \frac{\boldsymbol{E}_t A\cos(\theta_t)}{\boldsymbol{E}_r A\cos(\theta_r)} \tag{2.3.6}$$

Note that, since $\boldsymbol{E}_r/\boldsymbol{E}_t = (v_r\varepsilon_r\boldsymbol{\mathcal{E}}_{0r}^2/2)/(v_i\varepsilon_i\boldsymbol{\mathcal{E}}_{0i}^2/2)$, Eq. (2.3.5) becomes

$$\mathcal{R} = \left(\frac{\boldsymbol{\mathcal{E}}_{0r}}{\boldsymbol{\mathcal{E}}_{0i}}\right)^2, \tag{2.3.7}$$

while Eq. (2.3.6) gives:

$$\mathcal{T} = \frac{n_t\cos(\theta_t)}{n_t\cos(\theta_i)}\left(\frac{\boldsymbol{\mathcal{E}}_{0t}}{\boldsymbol{\mathcal{E}}_{0i}}\right)^2 \tag{2.3.8}$$

where we assumed that $\mu_i = \mu_t = \mu_0$ and we used the fact that $\mu_0 v_t\varepsilon_t = n_t/c$. Employing the total energy conservation, that is:

$$\boldsymbol{E}_i A\cos(\theta_i) = \boldsymbol{E}_r A\cos(\theta_r) + \boldsymbol{E}_t A\cos(\theta_t)\,, \tag{2.3.9}$$

it can be easily proved that:

$$\mathcal{R} + \mathcal{T} = 1\,. \tag{2.3.10}$$

The values $r = \left(\frac{\boldsymbol{\mathcal{E}}_{0i}}{\boldsymbol{\mathcal{E}}_{0i}}\right)$ and $t = \left(\frac{\boldsymbol{\mathcal{E}}_{0t}}{\boldsymbol{\mathcal{E}}_{0i}}\right)$ are called the amplitude coefficients. The intensity of the reflected and transmitted light depends not only on the angle of incidence but also on the polarization of the electromagnetic field. By convention, we refer to the polarization of electromagnetic waves as the direction of the electric field $\boldsymbol{\mathcal{E}}$, [6]. When $\boldsymbol{\mathcal{E}}$ is perpendicular to the plane of incidence, light is called s-polarized, while when $\boldsymbol{\mathcal{E}}$ is parallel to the plane of incidence, it is said that light is p-polarized. For s-polarized light the perpendicular components r_s and t_s of r and t are defined. For p-polarized light the parallel components r_p and t_p of r and t are given. Those coefficients are obtained considering the Maxwell's equations and the boundaries conditions due to the conservation of energy. For the first case (s-polarization), the boundaries conditions are given by the conservation of the tangent component of $\boldsymbol{\mathcal{E}}$ and of the normal component of $\boldsymbol{\mathcal{B}}$. For the second case (p-polarization), the boundaries conditions are given by the conservation of the tangential component $\boldsymbol{\mathcal{E}}$ and of the tangent component of $\boldsymbol{\mathcal{B}}$. These conditions together with Maxwell's equations lead to four equations with four unknowns. Solving those equations the Fresnel coefficients are derived. It is out of this work to show the details of Fresnel equations as they are widely explained in the leterature. In the following we provide Fresnel coefficients and we briefly explain their physical interpretation. We refer the reader to [7, 8] for more details. Fresnel's coefficients can also be derived using a different approach that does not involves Marxwell's equations, this method is widely explained in [9]. In case $\boldsymbol{E}$ is perpendicular to the plane of incidence the following results are obtained:

$$\begin{aligned} r_s &= \frac{n_i \cos(\theta_i) - n_t \cos(\theta_t)}{n_i \cos(\theta_i) + n_t \cos(\theta_t)} \\ t_s &= \frac{2 n_i \cos(\theta_i)}{n_i \cos(\theta_i) + n_t \cos(\theta_t)} \end{aligned} \tag{2.3.11}$$

In case $\boldsymbol{E}$ is parallel to the plane of incidence the amplitude coefficients are:

$$\begin{aligned} r_p &= \frac{n_t \cos(\theta_i) - n_i \cos(\theta_t)}{n_i \cos(\theta_t) + n_t \cos(\theta_i)} \\ t_p &= \frac{2 n_i \cos(\theta_i)}{n_i \cos(\theta_t) + n_t \cos(\theta_i)}. \end{aligned} \tag{2.3.12}$$

Using Snell's Law, Equations (2.3.11) and (2.3.12) are simplified as in the following:

$$\begin{aligned} r_s &= -\frac{\sin(\theta_i - \theta_t)}{\sin(\theta_i + \theta_t)} \\ r_p &= +\frac{\tan(\theta_i - \theta_t)}{\theta_i + \theta_t} \\ t_s &= -\frac{2 \sin\theta_t \cos\theta_i}{\sin(\theta_i + \theta_t)} \\ t_p &= +\frac{2 \sin\theta_t \cos\theta_i}{\sin(\theta_i + \theta_t)\cos(\theta_i - \theta_t)}. \end{aligned} \tag{2.3.13}$$

It can be show that

$$\begin{aligned} t_s + (-r_s) &= 1 \\ t_p + r_p &= 1 \end{aligned} \tag{2.3.14}$$

Fresnel coefficients are shown in Fig. 2.5 for the case in which light travels from a less dense to a more dense medium ($n_i < n_t$), that is external reflection. While in Fig. 2.6 the coefficients are shown for the case in which $n_i > n_t$, that is internal reflection. Note from Fig. 2.5 that r_p approaches to 0 when θ_i approaches to θ_p and it gradually decreases reaching -1 for an incident angle $\theta_i = 90°$. The angle θ_p is called Brewster's angle or polarization angle as only the component perpendicular to the incident ray will be reflected and therefore light is perfectly polarized. Similarly, Fig. 2.6 shows that $r_p = 0$ for $\theta_i = \theta_{p\prime}$. It can be show that $\theta_p + \theta_{p\prime} = 90°$. Fig. 2.6 also shows that r_p and r_s reach 1 when $\theta_i = \theta_c$. θ_c is called the critical angle. Light that hits the incident plane with an incident angle equal to or greater than the critical angle is totally reflected back and no transmitted light is observed. This phenomenon is called total internal reflection.

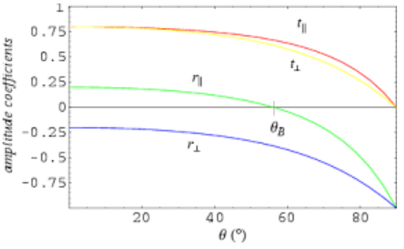

Figure 2.5: Amplitude coefficients of reflection and transmission as a function of the incident angle θ_i in the case of external reflection, i.e. $n_t < n_i$. ($n_t = 1$ and $n_i = 1.5$).

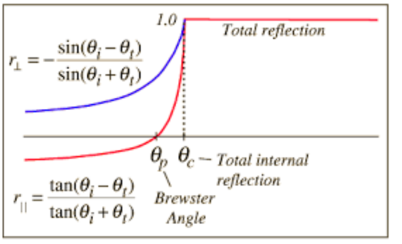

Figure 2.6: Amplitude coefficients of reflection as a function of the incident angle θ_i in the case of internal reflection, i.e. $n_t > n_i$. ($n_t = 1.5$ and $n_i = 1$).

The parallel and perpendicular components of $\mathcal{R}$ and $\mathcal{T}$ are:

$$\begin{aligned} \mathcal{R}_p &= r_p^2 \\ \mathcal{T}_p &= \frac{n_t \cos(\theta_t)}{n_t \cos(\theta_i)} t_p^2 \\ \mathcal{R}_s &= r_s^2 \\ \mathcal{T}_s &= \frac{n_t \cos(\theta_t)}{n_t \cos(\theta_i)} t_s^2 \end{aligned} \tag{2.3.15}$$

it can be show that

$$\begin{aligned} \mathcal{R}_s + \mathcal{R}_p &= 1 \\ \mathcal{T}_s + \mathcal{T}_p &= 1\,. \end{aligned} \tag{2.3.16}$$

For normal incidence, i.e. $\theta_i = 0$, there is no polarization and Eqs. (2.3.15) lead to:

$$\mathcal{R} = \mathcal{R}_p = \mathcal{R}_s = \left(\frac{n_i - n_t}{n_t + n_i}\right)^2 \tag{2.3.17}$$

and

$$\mathcal{T} = \mathcal{T}_p = \mathcal{T}_s = \frac{4 n_i n_t}{(n_t + n_i)^2}\,. \tag{2.3.18}$$

The behavior of the reflectance and transmittance is shown in Fig. 2.7

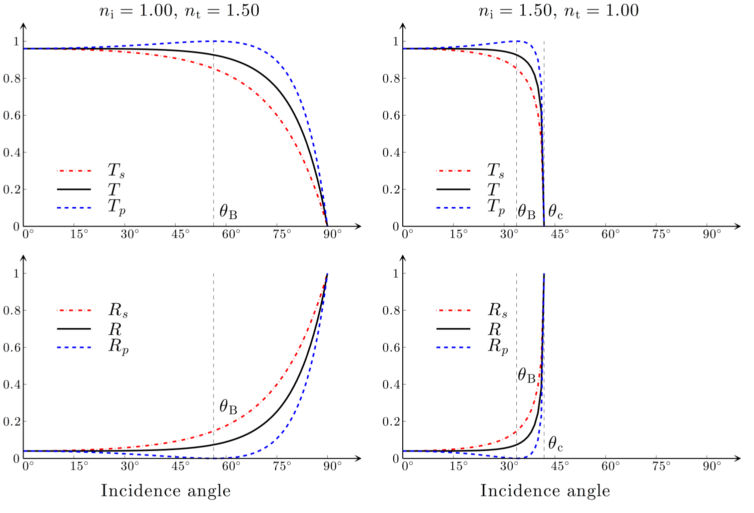

Figure 2.7: Top: Transmittance as a function of the incident angle both for the case of external reflection (top left) and internal reflection (top right).
Bottom: Reflectance as a function of the incident angle both for the case of external reflection (bottom left) and internal reflection (bottom right).

Chapter 3

Ray tracing

Ray tracing is a geometric problem that describes the transport of light within optical systems. It uses single rays to describe the propagation of light through an optical system. The influence of diffraction on the transport of a ray is neglected and geometrical modeling of an optical system is considered. Generally, the method can be implemented for two or more dimensions and for any optical system. In this thesis we restrict outself to two dimensional systems, therefore in the following a description of the ray tracing method 2D.

3.1 Ray tracing for two-dimensional optical systems

The ray tracing process consists of tracing each ray, which is considered to be a broken line, through a non-imaging system. Given a Cartesian coordinate system (x, z), a two-dimensional optical system symmetric with respect to the z-axis is defined. One of the simplest optical systems tha twe can image is the two-faceted cup, the profile of which is depicted in Fig. 3.1.

The light source $\mathsf{S}= [-a, a]$ (line 1) and the target $\mathsf{T} = \ [-b, b]$ (line 4) are two segments normal to the z-axis, where $a = 2$ and $b = 17$. The left and right reflectors (line 2 and 3) are oblique segments that connect the source and the target. All the optical lines i with $i \in \{1, \cdots, 4\}$ are located in air, therefore the refractive index $n_i = 1$ for every i. From now on, the coordinates $(x_i, z_i)_{i=1,\cdots,4}$ denote the intersection of the rays with line i and, $\boldsymbol{s}_i = (-\sin t_i, \cos t_i)$ is the direction vector of the rays that leave i, with t_i the angle that the ray forms with respect to the z-axis measured counterclockwise. As we consider only forward rays, the angles $t_i \in (-\pi/2, \pi/2)$. Therefore, a ray segment between (x_i, z_i) and (x_j, z_j) with $j \neq i$ is parameterized in real space by:

$$\boldsymbol{r}(s) = \begin{pmatrix} x_i - s\sin(t_i) \\ z_i + s\cos(t_i) \end{pmatrix} \qquad 0 \leq s \leq s_{\max}\,, \tag{3.1.1}$$

where s denotes the arc-length and $s_{\max}$ is the maximum value that it can assume.

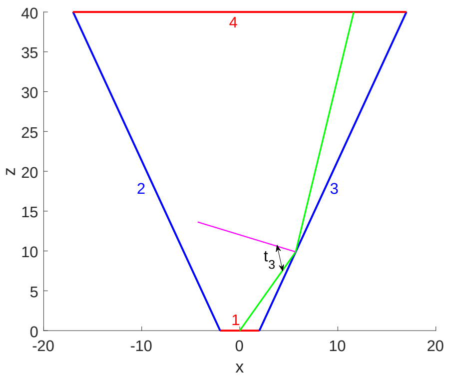

Figure 3.1: Shape of the two-faceted cup. Each line of the system is labeled with a number. The source S$= [-2, 2]$ (line number 1) is located on the x-axis. The target T$= [-17, 17]$ (line 4) is parallel to the source and is located at a height $z = 40$. The left and right reflectors (line 2 and 3) connect the source with the target.

3.2 Monte Carlo ray tracing

Assuming a Lambertian source, the input intensity at S emitted in the direction t_1 is given by:

$$I(t_1) = 2\mathrm{a}L\cos(t_1), \tag{3.2.1}$$

where L is the luminance and a is the half width of S. In order to compute the target intensity, we need to find a relation between the intensities at S and T. Hence, we need to know how the optical system influences the direction of the rays when they hit an optical line. To this purpose, the ray tracing procedure is often used in optics. Ray tracing relates the position coordinates (x_1, z_1) and the direction vector $\boldsymbol{s}_1$ of every ray at the source S with the corresponding position (x_4, z_4) and direction $\boldsymbol{s}_4$ at the target T. As in the following we will use often the target coordinates of the rays, from now on, to simplify the notation, we write t instead of t_4 and (x, z) instead of (x_4, z_4) for the target coordinates.

The ray tracing algorithm can be schematized as follows. For every ray that leaves S with initial position (x_1, z_1) and initial angle t_1, its ray parametrization is implemented according to Eq. (3.1.1). Then, the coordinates (x_i, z_i) of the intersection point between the ray and the line i that it hits are computed. The unit normal $\boldsymbol{\nu}_i$ to the line i at the point (x_i, z_i) is calculated to compute the change of direction of the ray. Since all the lines of the system are located in air, only the reflection law plays a role, [?]. Therefore, denoting with $\boldsymbol{t}_1$ the direction of the incident ray, the direction $\boldsymbol{t}_2$ of the reflected ray is given by:

$$\boldsymbol{t}_2 = \boldsymbol{t}_1 - 2(\boldsymbol{t}_1, \boldsymbol{\nu}_i)\boldsymbol{\nu}_i\,, \tag{3.2.2}$$

where the vectors $\boldsymbol{t}_1$ and $\boldsymbol{t}_2$ are unit vectors, [?]. The procedure explained above is repeated for every line that the ray encounters until it reaches the target and for every ray traced through the system.

There are different ways to implement the ray tracing procedure. An often used method is MC ray tracing which calculates the target photometric variables considering a sample of many rays that are traced randomly from S to T. The output intensity is computed as a function of the angular coordinate t and is calculated dividing the target into intervals of the same length, the so-called bins. A partitioning $P_1 : -\pi/2 = t_0 < t_1 < \cdots < t_{\mathrm{Nb}} = \pi/2$ of the interval $[-\pi/2, \pi/2]$ is defined where Nb is the number of bins in P_1. We remark that, with a slight abuse of notation, we indicated the angular coordinates of the rays at the target with t_j instead of $t_{4,j}$ for every $j \in \{0, \cdots, \mathrm{Nb}\}$. The normalized approximated intensity $g_{\mathrm{MC}}(t)$ is a piecewise constant function and its value over the j-th bin is the ratio between the number of rays that fall into that bin $\mathrm{Nr}[t_{j-1}, t_j)$ and the total number of rays traced $\mathrm{Nr}[-\pi/2, \pi/2]$. Hence, g_{MC} is defined by:

$$g_{\mathrm{MC}}(t) = \frac{\mathrm{Nr}[t_{j-1}, t_j)}{\mathrm{Nr}[-\pi/2, \pi/2]} \qquad \text{for } t \in [t_{j-1}, t_j). \tag{3.2.3}$$

Furthermore, the output intensity is computed from the value of the intensity $g_{\mathrm{MC}}(t_{j-1/2})$ along the direction $t_{j-1/2} = (t_{j-1} + t_j)/2$ for every bin $[t_{j-1}, t_j)_{j=1,\cdots,\mathrm{Nb}}$. The intensity $g_{\mathrm{MC}}(t_{j-1/2})$ gives an estimate of the probability that a ray reaches the target with an angle in the j-th interval $[t_{j-1}, t_j)$ of the partitioning P_1. This probability $\mathrm{P}_{j,\Delta t}$ is given by:

$$\mathrm{P}_{j,\Delta t} = \Pr(t_{j-1} \le t < t_j) = \frac{\int_{t_{j-1}}^{t_j} G(t)\mathrm{d}t}{\int_{-\pi/2}^{\pi/2} G(t)\mathrm{d}t}, \tag{3.2.4}$$

where $G(t)$ is the output intensity (not normalized) and it is measured in lumen per radian $[lm/rad]$. Note that $\sum_{j=1}^{\mathrm{Nb}} \mathrm{P}_{j,\Delta t} = 1$. Using the mean value theorem for the function $G(t)$ continuous in $[t_{j-1}, t_j]$, the integral at the numerator of the previous equation can be written as:

$$\int_{t_{j-1}}^{t_j} G(t)\mathrm{d}t = \Delta t\, G(t_{j-1/2}). \tag{3.2.5}$$

Hence, $\mathrm{P}_{j,\Delta t}$ is proportional to the size $\Delta t = (t_{\mathrm{Nb}} - t_0)/\mathrm{Nb}$ of the intervals, i.e., inversely proportional to the number of bins Nb of the partitioning P_1. Indicating with $\Phi = \int_{-\pi/2}^{\pi/2} G(t)\mathrm{d}t$ the total flux (measured in lumen $[lm]$), the error between the intensity $G(t_{j-1/2})$ and the averaged MC intensity $\Phi g_{\mathrm{MC}}(t_{j-1/2})/\Delta t$ is given by:

$$\begin{aligned} \left| G(t_{j-1/2}) - \frac{\Phi}{\Delta t} g_{\mathrm{MC}}(t_{j-1/2}) \right| \le& \\ &\left| G(t_{j-1/2}) - \frac{1}{\Delta t}\int_{t_{j-1}}^{t_j} G(t)\mathrm{d}t \right| + \\ &\frac{1}{\Delta t}\left| \int_{t_{j-1}}^{t_j} G(t)\mathrm{d}t - \Phi\, g_{\mathrm{MC}}(t_{j-1/2}) \right|. \end{aligned} \tag{3.2.6}$$

The first term of the right hand side of inequality (3.2.6) gives an estimate of how much the averaged intensity $\frac{1}{\Delta t}\int_{t_{j-1}}^{t_j} G(t)\mathrm{d}t$ differs from the exact intensity $G(t_{j-1/2})$. This term is due to the discretization of the target and therefore it depends on the number of bins Nb considered. Substituting $G(t)$ with its Taylor expansion around the point $t_{j-1/2}$ we obtain that this term is proportional to the square of the size of the bins, therefore the following equality holds:

$$\left|G(t_{j-1/2}) - \frac{1}{\Delta t}\int_{t_{j-1}}^{t_j} G(t)\mathrm{d}t\right| = \mathrm{C}_1/\mathrm{Nb}^2 \tag{3.2.7}$$

with $C_1 > 0$ a certain constant.

The second part of the right hand side of inequality (3.2.6) gives an estimate of the MC error and therefore it depends also on the number of rays traced. In order to show how this term decreases as a function of the number of rays traced, we define the random variable $X_j(t)$ as the variable that is equal to 1 if the ray with angular coordinate t is inside the interval $[t_{j-1}, t_j)$ and equal to 0 otherwise,

$$X_j(t) = \begin{cases} 1 & \text{if} \quad t \in [t_{j-1}, t_j), \\ 0 & \text{otherwise.} \end{cases} \tag{3.2.8}$$

The Bernoulli trial X_j follows a binomial distribution $B(1, \mathrm{P}_{j,\Delta t})$. Considering a sample of Nr rays, the variable $Y_j = \sum_{k=1}^{\mathrm{Nr}} X_j(t_k)$ follows a binomial distribution $B(\mathrm{Nr}, \mathrm{P}_{j,\Delta t})$, where t_k is the angle that the k-th ray forms with the optical axis. Then, using the de Moivre-Laplace theorem, we conclude that the variable Y_j is approximated by a normal distribution with mean value $E[Y_j] = \mathrm{Nr}\mathrm{P}_{j,\Delta t}$ and variance $\sigma^2[Y_j] = \mathrm{Nr}\mathrm{P}_{j,\Delta t}(1 - \mathrm{P}_{j,\Delta t})$ when a large number of rays is considered, see [**?**, **?**]. Thus, the normalized intensity along the direction $t_{j-1/2}$ is given by:

$$g_{\mathrm{MC}}(t_{j-1/2}) = \sum_{k=1}^{\mathrm{Nr}} X_j(t_k)/\mathrm{Nr}. \tag{3.2.9}$$

The mean value $E[g_{\mathrm{MC}}(t_{j-1/2})] = \mathrm{P}_{j,\Delta t}$ and the variance $\sigma^2[g_{\mathrm{MC}}(t_{j-1/2})] = \mathrm{P}_{j,\Delta t}(1 - \mathrm{P}_{j,\Delta t})/\mathrm{Nr}$. Note that the standard deviation $\sigma_j := \sigma[g_{\mathrm{MC}}(t_{j-1/2})]$ equals:

$$\sigma_j = \sqrt{\mathrm{P}_{j,\Delta t}(1 - \mathrm{P}_{j,\Delta t})/\mathrm{Nr}} = \frac{\mathrm{C}_2}{\sqrt{\mathrm{NbNr}}}\,, \tag{3.2.10}$$

for some $\mathrm{C}_2 > 0$. σ_j can be used to give an estimate of the difference between the intensity $g_{\mathrm{MC}}(t_{j-1/2})$ and its mean value $\mathrm{P}_{j,\Delta t}$. Therefore, the second term of the right hand side of relation (3.2.6) becomes:

$$\begin{aligned} &\frac{1}{\Delta t}\left|\int_{t_{j-1}}^{t_j} G(t)\mathrm{d}t - \Phi\, g_{\mathrm{MC}}(t_{j-1/2})\right| = \\ &\qquad \frac{\Phi}{\Delta t}\left|\mathrm{P}_{j,\Delta t} - g_{\mathrm{MC}}(t_{j-1/2})\right| \propto \\ &\frac{\Phi}{\Delta t}\sigma_j[g_{\mathrm{MC}}(t_{j-1/2})] = \mathrm{C}_3\frac{\mathrm{Nb}}{\sqrt{\mathrm{NbNr}}} = \mathrm{C}_3\sqrt{\frac{\mathrm{Nb}}{\mathrm{Nr}}}\,, \end{aligned} \tag{3.2.11}$$

for some $\mathrm{C}_3 > 0$, where the approximation holds because σ_j gives a measure for the error between $g_{\mathrm{MC}}(t_{j-1/2})$ and the probability $\mathrm{P}_{j,\Delta t}$, [**?**]. The second equality follows from Eq. (3.2.10). To conclude, the MC error over the j-th bin is estimated by:

$$\left|G(t_{j-1/2}) - \frac{\Phi}{\Delta t} g_{\mathrm{MC}}(t_{j-1/2})\right| = \frac{\mathrm{C}_1}{\mathrm{Nb}^2} + \mathrm{C}_4\sqrt{\frac{\mathrm{Nb}}{\mathrm{Nr}}}, \tag{3.2.12}$$

for $C_4 > 0$. Considering a fixed number of rays, we obtain that the minimal error is reached when $Nb \approx Nr^{1/5}$. Hence, if 10^{10} rays are considered the target has to be divided into 10^2 bins to minimize the MC error. This leads to computational efforts resulting in a very slow procedure.

Chapter 4

Ray tracing on phase space

4.1 Phase space concept

4.2 The edge-ray principle

4.3 Phase space ray tracing

Chapter 5

Two different appoaches to compute the boundaries in target phase space

5.1 The α-shapes approach

Given a finite set $\mathcal{S}$ of points we want to determine the shape formed by these points. α-shapes are geometrical objects which give us a good approximation of the shape of a given point set $\mathcal{S}$. Before giving a formal definition we explain an intuitive interpretation of α-shapes. As mentioned in [10] we can think of an α-shape as a mass of ice-cream with several chocolate pieces. The mass making up the space $\mathbb{R}^3$ and the chocolate pieces are the point set $\mathcal{S}$. Then the aim is to find the shape formed by the chocolate pieces. We can use a spoon with a spherical shape and carve out all parts of the ice-cream without removing the chocolate pieces. We will obtain a shape formed by arcs and points (see figure below for the two-dimensional case). Straightening the arcs to triangles and line segments we have an intuitive description of what is called the α-shape of $\mathcal{S}$. In our example, the parameter α determines of the radius of the carving spoon. If α is equal to 0 the shape degenerates to the point set $\mathcal{S}$. On the other hand, when $\alpha \to \infty$ the α-shape is simple the convex hull. More precisely the process is summarized as follows. Given a point cloud $\mathcal{S}$ we start with a triangulation of it (a possible choice could be the Delaunay triangulation described in the next section). For each triangle we calculate the radius of the circumcircle. If the radius is larger that α the triangle is removed from the shape. The rule of the parameter α is highly significant in this procedure. Hence we have to choose it in such a way to get a better approximation. The choice of the parameter α is closely related to the radius of the circumcircles. A possible strategy is to find the radius of the greater empty circumcircle. Thus α is related to the density of the points. In particular we have:

$$\alpha = C\frac{1}{\Delta}\ , \tag{5.1.1}$$

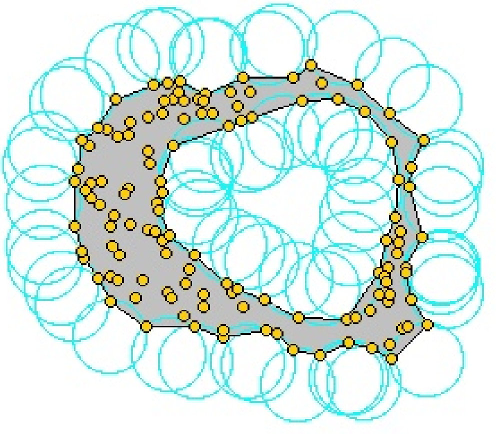

Figure 5.1: Construction of α-shape given a set of points in $\mathbb{R}^2$.

with C a constant that can be determined by a simulation and Δ the density of the point set $\mathcal{S}$ defined as:

$$\Delta = \frac{N}{\text{surface area}}\,, \tag{5.1.2}$$

where N is the number of points in $\mathcal{S}$ and the surface area is the area inside the boundaries of the region formed by the points cloud. Hence Δ is a constant. As mentioned above to find the α-shape of a point cloud we need a triangulation and a possible choise could be the Delaunay triangulation. As explained in [11] we can see a Delaunay triangulation as the dual of a Voronoi diagram. Let us define a Voronoi diagram in a metric space.

Definition 5.1.1. Let X be a space endowed with a distance d and $\mathcal{S} = \{S_1, \cdots, S_n\}$ a set formed by subsets of X. The Voronoi cell R_k associated with the set S_k where $k \in \{1, \cdots, n\}$ is defined as follows:

$$R_k = \{\mathbf{x} \in X \mid \mathrm{d}(\mathbf{x}, S_k) \leq \mathrm{d}(\mathbf{x}, S_j) \quad \forall j \neq k\}\,, \tag{5.1.3}$$

where $\mathrm{d}(x, A) = \inf\{\mathrm{d}(x, a) \mid a \in A\}$. The Voronoi diagram is defined as the tuple of the cells $(R_k)_{k\in\{1,\ldots,n\}}$ that are assumed to be disjoint.

The simplest case that we can have is the two-dimensional case that is the case where $X = \mathbb{R}^2$. The tuple $\mathcal{S} = \{1, \cdots, n\} \subset \mathbb{R}^2$ is now a set of points. The Voronoi diagram of $\mathcal{S}$ is a subsection of $\mathbb{R}^2$ such that every other region around a point $p \in \mathcal{S}$ contains all points that are closer to p than to every point in $\mathcal{S}$. A triangulation of the point set $\mathcal{S}$ is a set of edges $\mathcal{E}$ whose extremes are points of $\mathcal{S}$ such that the faces of each triangle are bounded by three edges and any edge that is not in $\mathcal{E}$ intersects one of the existing edges. The Delaunay triangulation is the dual graph of the Voronoi diagram: it consists of vertices (the points in $\mathcal{S}$) and it has an edge between two vertices if the two corresponding faces share an edge.
The Delaunay triangulation triangulates the convex hull of the point set $\mathcal{S}$. Instead,

the α-shape of a point set is formed only by the triangles (taken from the Delaunay triangulation) that satisfy the "α-test" and therefore is a suitable method to reconstruct the surface formed by a point cloud. Even if α-shapes are a powerful tool to reconstruct surfaces, some simulations show that there exist surfaces that are not described well by α-shapes. Indeed for some particular surface there exist no value of α that includes all desired triangles and deletes all undesired triangles. For instance, since the parameter α depends on the density of the point cloud, is intuitively clear that using α-shapes for a non-uniform points set we won't get a good approximation of the surface. Furthermore, the α-shape method doesn't work well when there is a sharp turn or a joint. In this case α-shapes often give a "webbed-foot" appearance at such joints since they improperly connect the adjacent surfaces. Hence a generalization of "classical" α-shapes is required. In the next section a method to solve the "density problem" for two separated and close objects is described. In [12] Teichmann and Capps present "Density-scaled α-shapes". The first step of this method is to make a triangulation of the point cloud. Then the key idea is to compute somehow the point-density of each point and use this to get an approximation of the point density of a triangle. In this way one can reduce the α-value in areas where the triangle's point density (see equation 5.1.6 for the definition) is higher than average in such a way that is possible to obtain a finer level of detail for areas that have an higher density. More precisely, each point $\mathbf{p} \in \mathcal{S}$ has a local point density defined as

$$\delta(\mathbf{p}) = \sum_{\mathbf{q}\in\mathcal{S}} \left(1 - \frac{\mathrm{d}(q,p)}{\lambda}\right) \qquad \forall \mathbf{q} \;\text{ such that }\; \mathrm{d}(\mathbf{p},\mathbf{q}) < \lambda\,, \tag{5.1.4}$$

where λ is the constant radius of the local neighborhood and $\mathrm{d}(\mathbf{x},\mathbf{y})$ is the Euclidean distance. When local density is larger than the average, that is when

$$\delta(\mathbf{p}) > \frac{1}{|\mathcal{S}|} \sum_{\mathbf{q}\in\mathcal{S}} \delta(\mathbf{q}) \tag{5.1.5}$$

we know some properties about the region surrounding $\mathbf{p}$. For instance, if the point set is uniformly distributed then it is possible to find areas with a high-density in the case where there are two closely separated surfaces. In point sets of non-uniform distribution, high densities are found when the surface presents a joint discontinuity. The algorithm developed by Teichmann and Capps is structured as follow. After computing density information for each point they make a triangulation of the point set. Then they calculate the average density $\delta(t)$ for each triangle Δ_{abc} defined as:

$$\delta(t) = \frac{\delta(a) + \delta(b) + \delta(c)}{3\mu}\,, \tag{5.1.6}$$

where μ is the global average density of the entire point set $\mathcal{S}$. If $\delta(t)$ is greater than 1 the density of the point cloud is higher. Hence is necessary to define another value of α:

$$\alpha\,' = \frac{\alpha}{\delta(t)^{\sigma}} \tag{5.1.7}$$

where σ is a value that is adjusted by the user. If δ is less than 1 the α-value is not modified. In this way it is possible to have a finer precision on the shape formed by the point set where the density is higher than the average density. Hence it is possible to distinguish two separated objects with different density.

5.2 The two-faceted cup

5.3 Results for a TIR collimator

5.4 The triangulation refinement approach

5.5 The two-faceted cup

5.6 Results for a TIR collimator

5.7 Results for a Parabolic reflector

5.8 Results for the Compound Parabolic Concentrator (CPC)

Chapter 6

The inverse ray mapping method: analytic approach

6.1 Explanation of the method

6.2 The two-faceted cup

6.3 The multi faceted cup

For two-dimensional systems every ray in the PS of a line is given by a two-tuple point. Therefore, the PS of every line is a two-dimensional space. The position coordinate in the PS of line i is the x-coordinate of the intersection point between the ray and the line i. The direction coordinate is the sine of the angle that the ray forms with respect to the normal of the line i multiplied by the index of refraction of the medium in which the ray is located. Let's now introduce some notation before explaining the details of the method. We indicate the PS with $S = Q \times P$, where Q is the set of the position coordinates q and P is the set of the direction coordinates $p = n \sin \tau$ with τ the angle between the ray and the normal $\boldsymbol{\nu}$ of the line and n is the index of refraction of the medium in which the line is located.

6.4 Results for the two-faceted cup

6.5 Results for the multi-faceted cup

6.6 Discussions

Chapter 7

The extended ray mapping method

7.1 Explanation of the method

7.2 Bisection procedure

7.3 Results for a parabolic reflector

7.4 Results for two different kind of TIR-collimators

Chapter 8

Extended ray mapping method to systems with Fresnel reflection

Chapter 9

Discussion and conclusions

Summary

I have changed the summary

38

Curriculum Vitae

Acknowledgments

Bibliography

[1] E. F. Zalewski, "Radiometry and photometry," *Handbook of optics*, vol. 2, pp. 24–1, 1995.

[2] J. Chaves, *Introduction to nonimaging optics.* CRC press, 2015.

[3] A. V. Arecchi, R. J. Koshel, and T. Messadi, "Field guide to illumination," SPIE, 2007.

[4] H. Zhu and P. Blackborow, "Etendue and optical throughput calculations," *Energetiq Technology, Inc., Woburn, MA*, 2011.

[5] P. H. Jones, O. M. Maragò, and G. Volpe, *Optical tweezers: Principles and applications.* Cambridge University Press, 2015.

[6] R. P. Feynman, "Feynman lectures on physics. volume 2: Mainly electromagnetism and matter," *Reading, Ma.: Addison-Wesley, 1964, edited by Feynman, Richard P.; Leighton, Robert B.; Sands, Matthew*, 1964.

[7] M. Born and E. Wolf, *Principles of optics: electromagnetic theory of propagation, interference and diffraction of light.* Elsevier, 2013.

[8] E. Hecht, *Optics.* Parson Addison-Wesley, 2002.

[9] R. P. Feynman, R. B. Leighton, and M. Sands, *The Feynman lectures on physics, Vol. I: The new millennium edition: mainly mechanics, radiation, and heat*, vol. 1. Basic books, 2011.

[10] H. Edelsbrunner and E. P. Mücke, "Three-dimensional alpha shapes," *ACM Transactions on Graphics (TOG)*, vol. 13, no. 1, pp. 43–72, 1994.

[11] J. Portegies and P. Lighting, "Fast ray tracing in phase space for optical design," 2013.

[12] M. Teichmann and M. Capps, "Surface reconstruction with anisotropic density-scaled alpha shapes," in *Visualization'98. Proceedings*, pp. 67–72, IEEE, 1998.